Functional characterisation of the type 1 von Willebrand disease candidate *VWF* gene variants: p.M771I, p.L881R and p.P1413L

Ergul Berber[1], Mehmet Ozbil[1], Christine Brown[2], Zafer Baslar[3], S. Hande Caglayan[4], David Lillicrap[2]

[1]*Department of Molecular Biology and Genetics, Istanbul Arel University, Istanbul, Turkey;* [2] *Department of Pathology and Molecular Medicine, Queen's University, Kingston, Canada;* [3]*Department of Internal Medicine, Cerrahpasa Medical Faculty, Istanbul University, Istanbul;* [4]*Department of Molecular Biology and Genetics, Boğaziçi University, Istanbul, Turkey*

Background. Abnormalities in the biosynthetic pathway or increased clearance of plasma von Willebrand factor (VWF) are likely to contribute to decreased plasma VWF levels in inherited type 1 von Willebrand disease (VWD). Recent studies demonstrated that 65% of type 1 VWD patients have candidate *VWF* mutations, the majority of which are missense variants. The purpose of this study was to explore the effects of three *VWF* missense mutations (p.M771I, p.L881R and p.P1413L) located in different functional domains of VWF, reported as candidate mutations in type 1 VWD patients in the course of the MCMDM-1VWD study.

Materials and methods. The focus of these studies was on the intracellular biosynthetic processing and localisation of VWF in a heterologous cell system. Molecular dynamic simulation for p.M771I and p.P1413L was also performed to analyse the conformational effects of the changes.

Results. As determined by immunofluorescence antibody staining and confocal microscopy of HEK293 cells, the intracellular localisation of recombinant VWF with the p.M771I variation was impaired. Transient transfection studies and phorbol myristate acetate stimulation in COS-7 cells revealed significant intracellular retention. In addition, major loss of VWF multimers was observed for only the p.M771I mutation. Molecular dynamic simulations on p.M771I mutant VWF revealed distinct structural rearrangements including a large deviation in the E' domain, and significant loss of β-sheet secondary structure.

Discussion. The pathogenic effects of candidate *VWF* gene mutations were explored in this study. *In vitro* expression studies in heterologous cell systems revealed impaired secretion of VWF and a dominant negative effect on the processing of the wild-type protein for only the p.M771I mutation and none of the mutations affected the regulated secretion.

Keywords: type 1 VWD, *VWF* gene, VWF, Weibel-Palade bodies, von Willebrand disease.

Introduction

von Willebrand factor (VWF) is a multimeric glycoprotein that maintains haemostasis in the vascular system by serving as a carrier of coagulation factor VIII and mediating platelet plug formation at the site of vascular injury[1]. VWF is secreted mainly from endothelial cells. During its biosynthesis VWF undergoes a series of post-translational modifications and some of the newly synthesised protein is released constitutively. The remainder of the protein is stored for regulated release from cytoplasmic storage granules, Weibel-Palade bodies[2,3]. Weibel-Palade bodies store the highest molecular weight VWF multimers, which are released upon stimulation by natural agonists, such as thrombin, or the synthetic vasopressin analogue, DDAVP[4]. Abnormalities in the biosynthetic pathway or increased clearance of plasma

VWF are likely to contribute to decreased plasma VWF levels. Inherited partial deficiency of VWF is classified as type 1 von Willebrand disease (VWD), which is characterised by a mild to moderate decrease in plasma VWF levels[5,6].

Type 1 VWD accounts for about 60-80% of the cases of the disease. However, the clinical diagnosis of type 1 VWD is complicated by the incomplete penetrance and variable expression of the abnormal VWF phenotype. VWF levels range from 5 to 40% in type 1 VWD, depending on the molecular pathogenesis of the disease[7]. The molecular basis of type 1 VWD remains incompletely understood. Recent studies of about 500 patients with type 1 VWD revealed that 65% had candidate *VWF* gene mutations, most of which were missense mutations[8-10]. In order to understand the molecular pathogenesis of type 1

VWD better, an examination of whether the missense variants are pathogenic or polymorphic is necessary.

The purpose of the present study was to explore the effect of three *VWF* missense mutations (p.M771I, p.L881R and p.P1413L), which were reported to be candidate mutations in type 1 VWD patients in the course of the Molecular and Clinical Markers for the Diagnosis and Management of type 1 von Willebrand Disease (MCMDM-1VWD) study and listed as mutations in the International Society of Thrombosis and Haemostasis Scientific and Standardization Committee (ISTH SSC) VWF database[9,11]. These mutations are located within the D', D3 and A1 domains of VWF, respectively. The D' domain is involved in multimer formation and factor VIII (FVIII) binding. The D3 domain is responsible for FVIII binding. The A1 domain is involved in platelet association. Thus, expression analysis of the candidate mutations would reveal the effect of those domains in the pathogenesis of VWD in these patients. Furthermore, by applying computational methods we investigated the effect of the p.M771I mutation (which lies in the FVIII binding region) at the molecular level. We describe a detailed biosynthetic analysis of VWF associated with the three VWF variants to determine how these mutations interfere with the biosynthesis, intracellular storage, secretion and structure of VWF.

Materials and methods
Mammalian cell cultures

COS-7 cells (ATCC, Manassas, VA, USA) and HEK-293 cells (ATCC) were cultured in complete Dulbecco's modified Eagle's medium at 37 °C in 5% CO_2.

In vitro mutagenesis of von Willebrand factor

The *VWF* gene variants were introduced into the pCIneo-hVWF expression vector using the QuikChange MultiSite-Directed Mutagenesis kit (Stratagene, La Jolla, CA, USA). The 4132bp long XbaI-EcoRI fragment of the human *VWF* cDNA sequence from the pCIneo-hVWF expression vector was subcloned into pBluescript expression vector using mutagenic primer pairs. The mutated fragments were ligated back into the pCIneo-hVWF expression vector to create the pCIneo-hVWF-mutant constructs. Mutant constructs were made for p.M771I (D'-mutant), p.L881R (D3-mutant) and p.P1413L (A1-mutant). The mutant cDNA was sequenced to confirm the presence of the mutated nucleotide and the sequence integrity of the remaining VWF cDNA construct.

Transient von Willebrand factor expression studies

COS-7 and HEK-293 cells were transfected with either pCIneo-hVWF-WT or pCIneo-hVWF-mutant vectors (4 µg) alone by using Fugene X-tremeGene HP DNA transfection reagent (Roche, St. louis, MO, USA). The cells were also co-transfected with pCIneo-hVWF-WT and pCIneo-hVWF-mutant vectors in equal amounts (2 µg, each) to mimic the heterozygous state. Forty-eight hours after transfection, media were collected and cells were lysed. The amount of VWF present in the media and cell lysates was determined at Istanbul University Cerrahpasa Hospital Blood Unit using a BCS XP (Behring Siemens, Erlangen, Germany).

Stimulated release of von Willebrand factor from transfected cells

Forty-eight hours after transfection, HEK-293 cells expressing VWF were rinsed with phosphate-buffered saline and then incubated with calcium-free Hank's buffered salt solution in the absence or presence of 100 nM phorbol myristate acetate (PMA) for 30 minutes. The amount of recombinant VWF secreted into the incubation medium was determined at Istanbul University Cerrahpasa Hospital Blood Unit using a BCS XP (Behring Siemens).

Confocal immunofluorescence microscopy

To evaluate the intracellular location of VWF in transfected HEK-293 cells, the cells were analysed by immunofluorescence antibody staining and confocal laser scanning microscopy (Leica TCS SP2 multi photon, Wetzlar, Germany). Forty-eight hours after transfection, the cells were fixed in formalin, permeabilised in 1% Triton X-100 on ice and incubated in a serum-free blocking buffer for 20 minutes. They were incubated with a primary anti-VWF antibody (Dako, Glostrup, Denmark) at 4 °C for 16 hours. Then, FITC-labeled secondary antibody (Dako) was applied for 1 hour and the cells were mounted with Vectashield mounting medium.

Multimer analysis

To analyse the effects of the selected *VWF* gene variations on VWF multimer structure, multimer analysis was performed for the recombinant VWF expressed in HEK-293 cells in a homozygous state. A 1.4% sodium dodecyl sulphate agarose gel was used to determine the multimeric structure of the VWF mutants. The multimers were visualised by chemiluminescent-based imaging using a horse-radish peroxidase conjugated polyclonal rabbit anti-human VWF antibody P0226 (Dako).

Molecular dynamic simulations

The structural effects of p.M771I and p.P1413L at the molecular level were investigated by simulations of molecular dynamics (MD) on both wild-type (WT) and mutated VWF. The other two mutations could not be tested *in silico* because of the lack of three-dimensional structures. MD simulations on the FVIII

binding site and the A1 domain of human VWF were performed using the GROMACS 4.0.7 programme[12,13] (Science for Life Laboratory, Stockholm University and KTH, Stockholm, Sweden) with the GROMOS force field GROMOS96 53A6[14]. Initial coordinates for WT VWF were taken from the solution NMR structure (PDB ID: 2MHP)[15] and initial coordinates for p.M771I mutated VWF simulations were prepared using VMD software (NIH Center for Macromolecular Modeling and Bioinformatics, at the Beckman Institute, University of Illinois at Urbana-Champaign, Urbana and Champaign, IL, USA)[16] . Similarly, initial coordinates of the A1 domain of WT-VWF were taken from the X-ray structure (PDB ID: 4C2A) and the structure of p.P1413L-mutated VWF was prepared in VMD software. All VWF systems were placed in a truncated cubic box with dimensions of 82.0×44.0×44.0 Å. These dimensions ensure that at any point of the simulation proteins stay in the simulation box. The box was filled with single point charge water molecules[17] and some of them were displaced during the addition of chloride ions to neutralise the system (Supplementary Figure 1A).

The starting structures were subsequently energy-minimised using the steepest descent method for 50,000 steps. The energy-minimised structures were taken for the production phase. The MD simulations without any constraints were carried out using a constant number of particles (N), pressure (P) and temperature (T) i.e. NPT ensemble. The SETTLE algorithm was applied to constrain the bond length and bond angle of the water molecules[18], while the LINCS algorithm was used to constrain the bond length of the peptide[19]. The long-range electrostatic interactions were calculated with the particle-mesh Ewald method[20]. A constant pressure of 1 bar was applied with a coupling constant of 1.0 ps and water molecules/chloride ions were coupled separately to a bath at 300 K with a coupling constant of 0.1 ps. The equation of motion was integrated at 2 fs time steps using a leap-frog algorithm[21]. Production runs were run for 5 ns. The tools available in the GROMACS programme package and VMD software were used to analyse the MD trajectories.

Results
In vitro expression analysis in COS-7 cells
The effect of the mutations on the biosynthesis of the recombinant VWF was analysed in COS-7 cells. The expression vectors pCIneo-hVWF-WT (wild type) and the expression vector carrying the candidate mutations were transiently transfected into COS-7 cells alone or together to generate wild-type, mutant homozygous and heterozygous genotypes, the last condition mimicking the status of type 1 VWD patients. To determine whether the mutant recombinant protein was retained within cells or was efficiently secreted, VWF:Ag levels were assayed in cell lysates and in the conditioned media. *In vitro* expression studies demonstrated a significant increase in the amount of VWF in the cell lysate only with 771I mutation in the homozygous state. The other candidate mutations, 881R and 1413L, did not interfere with the secretion of the recombinant protein significantly in COS-7 cells. Furthermore, a significant decrease in recombinant VWF secretion was only observed in COS-7 cells co-transfected with 771I and WT constructs in a 1:1 ratio (Figure 1A, B).

In vitro expression analysis in HEK-293 cells
In order to test the responsiveness of the storage granules formed in HEK-293 cells by the mutant recombinant constructs in homozygous and heterozygous states, the cells were stimulated with PMA, which stimulates protein kinase C-mediated exocytosis from these organelles. Pseudo-Weibel-Palade bodies formed by the mutant constructs were sensitive to stimulation in both states, resulting in increased VWF secretion (Figure 1C).
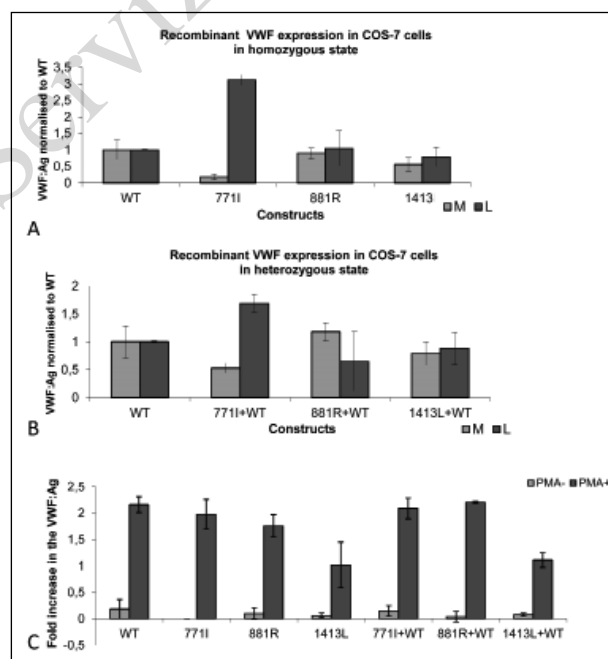

Figure 1 - (A) Recombinant VWF levels in media and lysates. Transfection of wild-type (WT) and mutant plasmids alone (n=3) to mimic the homozygous state.
(B) Recombinant VWF levels in media and lysates. Co-transfection of WT and mutant plasmids in a 1:1 ratio (n=3) to mimic the heterozygous condition.
(C) Stimulant sensitivity of pseudogranules formed by WT and mutant constructs alone or WT and mutant co-transfection in HEK-293 cells.
VWF: von Willebrand factor; VWF:Ag: VWF:Antigen; PMA: phorbol 12-myristate 13-acetate; M: media, L: lysate.

Immunofluorescent staining of von Willebrand factor in transfected HEK293 cells

In order to determine the effect of the selected, candidate *VWF* gene mutations on the storage of the recombinant VWF, immunofluorescent staining was performed in the transfected HEK-293 cells.

Immunofluorescent staining of the HEK-293 cells transfected with mutant constructs demonstrated that the p.M771I mutation caused impaired intracellular storage in the cells transfected with the mutant construct alone which mimics the homozygous state. In contrast, a normal pattern of intracellular storage was observed for the VWF variants with the p.L881R and p.P1413L changes in the homozygous state (Figure 2).

Computational investigation of the p.M771I mutation on von Willebrand factor structure

Structural comparison of WT VWF and the mutated VWF obtained from 5 ns long MD simulations revealed significant alterations. The secondary structures obtained from the most representative structures from each simulation revealed that the mutation decreased β-sheet content significantly, i.e. by 4.0% (β-sheet, random coil for WT [PDB ID: 2MHP] is 29.3 and 55.6, respectively and 25.3 and 55.6 for p.M771I mutated, respectively). A 4.0% decrease in β-sheet content indicates loss of rigidity, thus leading to a more flexible structure. Any significant change (increase or decrease) in secondary structure contents will change the topology of the domain thus affecting its biological function. Increasing flexibility might be an important obstacle to FVIII binding to the TIL' domain.

The vast majority of this loss occurred in the TIL' domain, specifically around the mutation site. WT protein possessed β-sheet structures at residues p.Met771-p.Leu774 and Gly807-Leu809, whereas p.M771I mutated protein only displayed Leu774 and Gly807 in the β-sheet structure. A strong hydrogen bond between NH_{Gly}-O_{Leu} (2.1 Å) brings two amino acids together and create an anti-parallel β-sheet, although
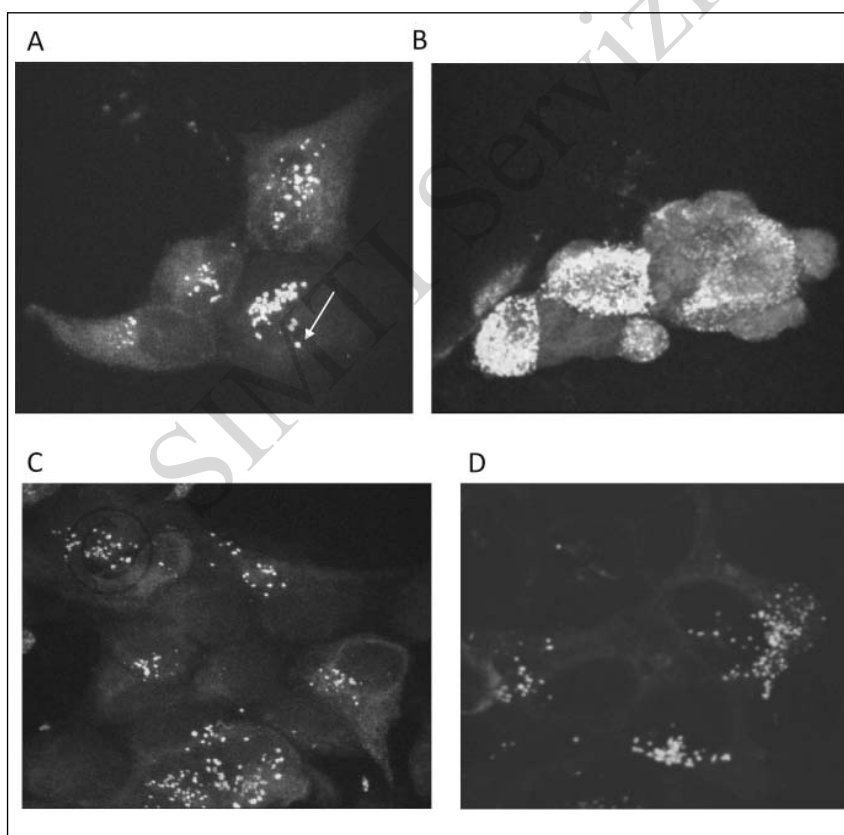

Figure 2 - Intracellular localisation of VWF in transfected HEK293 cells was analysed by immunofluorescence antibody staining and confocal laser scanning microscopy.
Cells were immunolabelled with FITC-labelled anti-human VWF antibody and, for cytosolic actin filaments, with Alexa Fluor 647 phalloidin. Immunofluorescence staining of HEK293 cells transfected with: (A) wild-type VWF; (B) 771I mutant VWF plasmid; (C) 881R mutant VWF plasmid, and (D) 1413L mutant VWF plasmid. The arrow indicates a pseudo Weibel-palade body.
FITC: fluorescein isothiocyanate; VWF: von Willebrand factor.

it is formed by single amino acid strands. Conversion of the β-sheet secondary structure into a random coil conformation in the mutation site region of the TIL' domain clearly indicated the local effect of the mutation. In the context of this local effect, we also observed alterations of intermolecular interactions. Hydrogen bonding between the backbone N atom of p.M771 and H atom of Leu 809 disappeared upon the mutation. A possible reason for this alteration might be the increased hydrophobicity caused by the Met to Ile substitution. It was also observed that the side chain of the Ile771 residue pushed water molecules further. The average number of water molecules within 5 Å of Met771 was 11 throughout the simulation whereas it was eight for Ile771. This reduction resulted in fewer water molecules available for hydrogen bonding with VWF protein. This was not unexpected, as it is known that although both M and L residues are non-polar, the sulphur atom in the Met residue can facilitate hydrogen bonding[22]. The direct result of this loss of hydrogen bonding and increased hydrophobicity was the loss of β-sheet character at this region. This structural rearrangement might lead to an impairment in FVIII binding. The patient's reduced level of FVIII also suggests impairment in FVIII; there were, however, no information on the patient's VWF:FVIIIB.

Calculation of root mean square (RMSD) values for each amino acid throughout 5 ns simulations revealed that there was a significant increase in individual RMSD values for E' domain residues. RMSD values are the measure of the average distance between the backbone atoms of the initial structure and structures at each 0.02 ps time interval. Supplementary Figure 1B shows significant increases starting from residue Cys810 with the p.M771I mutation. These large deviations were confirmed by the hinge-like motion of the E' domain moving closer to the TIL' domain. A decrease in inter-molecular distances between C_A atoms of residues from two domains also displays this type of motion. A C_A atom is one the carbon atoms forming a protein backbone and to which a sidechain is attached. While looking at the hinge motion, distances between C_A atoms are selected for two reasons: (i) as they are located in the backbone, they represent the movement of amino acids and domains more accurately, (ii) they lack the flexibility of sidechain atoms, which may lead to inaccurate estimations due to their highly dynamic nature. Thus quantifying the hinge motion with backbone C_A atoms is more accurate and is commonly applied in the literature. These distances, for WT and in parentheses for p.M771I VWF protein, include Cys792-Pro828: 8.54 Å (7.26 Å), Cys792-Cys829: 8.43 Å (7.31 Å), and Gln793-Phe830: 8.04 Å (5.37 Å). These data indicate the global effect of the mutation on E' domain structure. These kinds of global structural effects upon mutations are well reported in the literature[23].

In contrast, the p.P1413L mutation in the A1 domain decreased individual RMSD values specifically in two regions, i.e. p.Leu1275-p.Glu1305 and p.Ser1345-p.Leu1365. These values are presented in Supplementary Figure 1C. Similar to what was observed for the p.M771I mutation, these regions do not include the mutation area (p.1413L). The distribution of secondary structure features (β-sheet, random coil) for WT (PDB ID: 4C2A) are 19.3 and 36.6, respectively; and 21.3 and 36.1 for p.P1413L, respectively, for mutated VWF protein.

Like the M771I mutation, the P1413L mutation also changes the secondary structure content of VWF protein compared to that of the WT protein. A 2% increase of β-sheet content will result in a more rigid A1 domain which might affect its functioning (platelet association). The global effect of the mutation can still be seen on the structure of the protein.

Multimer analysis of recombinant von Willebrand factor

Transfection with p.M771I-, p.L881R-, and p.P1413L-carrying recombinant constructs in COS-7 cells revealed the secretion of a full range of VWF multimers except for the p.M771I mutant construct (Figure 3).

Discussion

In this study we functionally characterised three *VWF* gene mutations (p.M771I, p.L881R and p.P1413L) that were identified in the MCMDM-1 VWD study[9] and listed as mutations in the ISTH-SSC VWF mutation database, using *in vitro* expression experiments. These variations were selected from different functional domains of VWF to analyse the functional effects of these specific amino acid alterations on the domain function. p.M771I, p.L881R are located within the D' region and D3 region, respectively, which are involved in FVIII binding. In addition, the D' region is implicated in multimer formation. p.P1413L is located within the A1 domain, which is responsible for platelet binding. These three *VWF* gene variants were detected in the MCMDM-1VWD study as type 1 VWD candidate mutations[10]. The three patients studied were reported to be heterozygous for the selected variations and have a normal multimer VWF structure with decreased VWF:Ag level (below 50%). The patient with the p.L881R variation was also a compound heterozygote for the p.N1421K mutation, while the other candidate mutations were the only *VWF* gene variations detected in the patients.

The VWF:Ag level was 38 IU/dL in the patient with the p.M771I variation and FVIII:C, VWF:RCo and VWF:CB levels were proportionally decreased in this
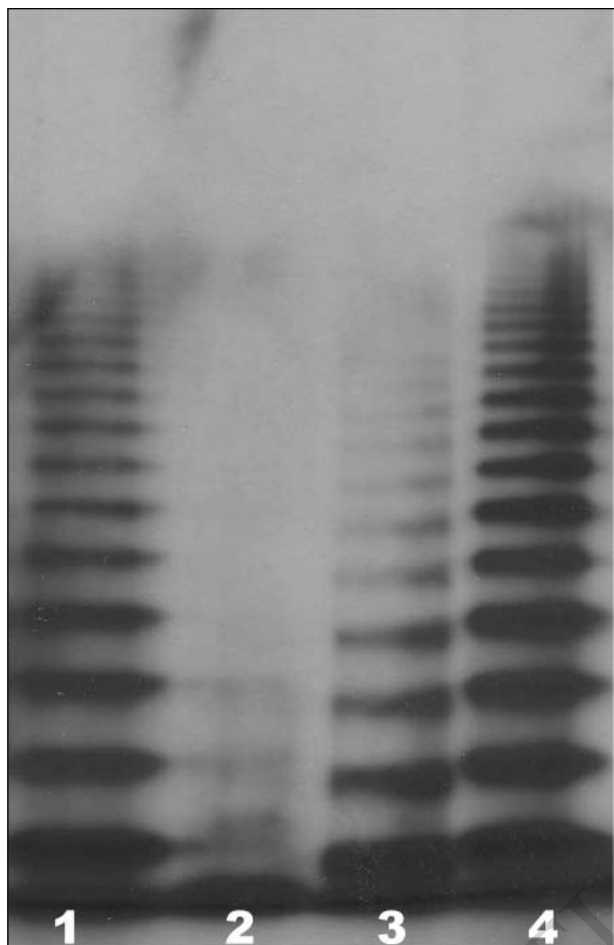
Figure 3 - Multimer analysis of recombinant VWF expressed in HEK-293 cells.
Lane 1 is 1413L mutant, lane 2 is 771I mutant, lane 3 is 881R mutant and lane 4 is wild-type recombinant VWF. VWF: von Willebrand factor.

patient (20 IU/dL, 59 IU/dL and 49 IU/dL, respectively) (Table I). The p.M771I variation is caused by the substitution of c.2313G by T. Alignment of *VWF* gene sequences of different species showed that c.2313G has been conserved among different species (*Homo sapiens, Mus musculus, Bos taurus, Sus scrofa, Canis lupus, Felis catus, Macaca malate*). *In vitro* expression studies in COS-7 cells demonstrated that the p.M771I variation causes marked intracellular retention and

impaired secretion of VWF. Co-transfection studies with WT VWF revealed the dominant-negative effect of the p.M771I variant. Although it did not affect the PMA-stimulated release of VWF in HEK-293 cells, it significantly impaired VWF intracellular storage in the pseudo-Weibel Palade bodies and interfered with normal multimer formation. The p.M771I variation is a missense change located within the D' region of VWF, which is implicated in multimer formation and Weibel Palade body storage in endothelial cells. Although Met and Ile are both hydrophobic amino acids, *in silico* analysis with SIFT and polyphen suggests that this variation is harmful. In addition, the patient's low FVIII level suggests that the p.M771I change might be associated with the type 2N phenotype by interfering with FVIII binding of mutant VWF. Hence MD analysis results also suggest impaired FVIII binding. However, we did not have information on the plasma FVIII:VWF binding assay and FVIII binding of the expressed mutation was not assessed.

Further MD simulations shed light on the structural effect of this mutation at the molecular level. We observed a significant decrease in β-sheet content, mainly in the TIL' region of the D' domain. This was the outcome of change in the hydrophobicity of this residue leading to a loss of hydrogen bonding between p.Met771 and p.Leu809. In addition to this local alteration, the p.M771I mutation was predicted to lead to structural rearrangement in the E' subdomain as well. The inter-molecular distances between two subdomains decreased significantly, and with hinge-like motion subdomain E' shifted towards the TIL' subdomain. In contrast, with the p.P1413L mutation, no significant structural rearrangements were observed. Generally the individual RMSD values for each residue decreased when compared to WT-VWF values; in two specific regions they decreased dramatically, i.e. p.Leu1275-Glu1305 and p.Ser1345-Leu1365. Our *in vitro* studies demonstrated that p.M771I is the cause of the type 1 VWD phenotype in patients, which was also confirmed with the large structural rearrangements observed in MD simulations unlike the negligible structural disruptions observed with the p.1413L mutation.

In vitro expression studies with the p.L881R and p.P1413L constructs in COS-7 cells demonstrated that

Table I - Phenotypic data of the type 1 VWD patients studied.

Patients' genotype	FVIII:C, IU/dL	VWF:RCo, IU/dL	VWF:Ag, IU/dL	VWF:CB, IU/dL	VWF:RCo/VWF:Ag
M771I heterozygous	20	59	38	49	1.55
L881R/N1421K heterozygous	30	3	27	22	0.11
P1413L heterozygous	58	39	44	37	0.89

VWD: von Willebrand disease; FVIII:C: FVIII activity; VWF:RCo: VWF ristocetin co-factor activity; VWF:Ag: VWF antigen; VWF:CB: VWF collagen binding.

neither of the variants affected VWF biosynthesis, secretion or multimer formation significantly. Besides, the variations did not show a dominant negative effect on the biosynthesis and secretion upon heterozygous transfection studies. PMA stimulation experiments in transfected HEK-293 cells demonstrated that these variations do not affect the stimulated release of the recombinant VWF from storage granules. In addition, p.L881R and p.P1413L variant recombinant VWF were observed to be localised in the apparently normal pseudo Weibel-Palade bodies.

The p so that the patient has reduced FVIII, VWF:Ag and VWF:CB levels.L881R variation was detected in a patient who was a compound heterozygote for p.N1421K mutation and had the following VWF indices: VWF:Ag 27 IU/dL, VWF:RCo 3 IU/dL, FVIII:C 30 IU/dL and VWF:CB 22 IU/dL (Table I). *In vitro* expression studies have shown that the p.N1421K mutation impairs the platelet binding of VWF. However, in this patient the VWF:RCo is lower than would be expected for a p.N1421K heterozygote. p.L881R is a non-conservative change from a hydrophobic amino acid to a hydrophilic amino acid within the D3 domain of VWF. The mutation substitutes G for T at nucleotide c.2642, which is highly conserved (*Homo sapiens, Mus musculus, Sus scrofa, canis lupus, Felis catus, Macaca malate*). Studies have shown that D'-D3 domains are involved in both FVIII binding and P-selectin binding which is required to anchor ultra-large VWF multimers to the activated endothelial cell surface and facilitate access to the A2 domain cleavage site for ADAMTS-13. The D3 domain is also involved in N-terminal disulfide linkages responsible for the generation of VWF multimers. Thus, in light of the patient's very low VWF:RCo level, it is suggested that the p.L881R variation may influence either multimer generation and/or multimer cleavage with the resultant abnormal VWF:RCo and VWF:CB levels. Nevertheless, it remains possible that the phenotype could represent the combined effects of both the p.L881R and p.N1421K variants.

The p.P1413L variant was detected in a patient with 44 IU/dL VWF:Ag, 58 IU/dL FVIII:C, 39 IU/dL VWF:RCo, and 37 IU/dL VWF:CB levels (Table I). The variation is a non-conservative change from a polar amino acid to non-polar amino acid in the A1 domain of VWF caused by a c.4238C>T substitution. The A1 domain contains the GPIBa binding site and *VWF* gene missense mutations within the A1 domain have been associated with type 2M VWD[9]. Proline has a conformational rigidity compared to other amino acids. Although a structural change was expected from this mutation, MD analysis did not show a significant structural reorientation in this domain.

Conclusions

The molecular pathogenesis of type 1 VWD is heterogeneous[24]. In addition to *VWF* gene variants, other genetic loci might affect VWF plasma levels. To date, the ABO blood type has been determined to be the major non-VWF genetic modifier of the plasma VWF:Ag level[7,25].

The *VWF* gene is highly polymorphic. In addition to coding sequence variants, single nucleotide variants are observed within the VWF promoter and they have been shown to affect VWF:Ag level[26]. A large number of non-synonymous coding polymorphisms have been observed within the *VWF* gene[27-30]. While some of these non-synonymous changes affect VWF biosynthesis, some of them have been found to be associated with a reduction in the VWF plasma level and some of them affect the response to desmopressin treatment. For example, the p.G160W variant was shown to cause markedly impaired secretion[10,31]. A common *VWF* gene variant, p.R924Q, has been shown to be associated with reduced VWF and FVIII levels in combination with blood type O[32,33]. Another common *VWF* gene variant, p.Y1584C, has been associated with increased ADAMTS-13-mediated cleavage[34-36]. In addition, it has been demonstrated that the p.R1205 residue has a role in macrophage-mediated VWF clearance[37] and finally, the p.R1374H and p.V1822G variants are associated with absent and partial responses to desmopressin, respectively[38]. Furthermore, some A3 domain *VWF* variants, such as p.W1745C, p.S1783A and p.H1786D, affect collagen binding without affecting multimer formation[39,40]. In addition, the p.1716P, p.C2190Y and p.R2663C *VWF* variants were shown to affect VWF secretion with loss of Weibel-Palade body formation[41] and p.Cys1149Arg was shown to cause intracellular retention and degradation of heterodimers[42].

Assessment of the pathogenic significance of non-synonymous *VWF* gene variants helps to improve our understanding of the molecular pathogenesis of type 1 VWD and also provides information to optimise treatment.

We have shown the pathogenic effect of one of the three missense *VWF* gene alterations. This study has also demonstrated the importance of *in vitro* expression studies to analyse the pathogenicity of candidate *VWF* gene mutations in accordance with other studies[31]. However, additional studies, fore example, of VWF survival[43], are also required to demonstrate definitive pathogenicity of candidate mutations.

In conclusion, although further studies are needed to elucidate the pathogenic effects of the p.L881R and p.P1413L variations, we have shown that p.M771I is the pathogenic alteration with a dominant negative effect by disturbing the structure of the D' domain according to MD simulation analysis.

Acknowledgements

Authorship contributions

EB performed *in vitro* site-directed mutagenesis studies, transient transfection analysis, immunofluorescent staining, analysed the data and wrote the manuscript; MO performed the MD simulation analysis; CB performed the multimer analysis; ZB performed the ELISA; SHC helped with the immunofluorescent staining and analysis; DL analysed the data and wrote the manuscript.

The Authors declare no conflicts of interest.

References

1) Ruggeri ZM, Ware J. The structure and function of von Willebrand Factor. Thromb Haemost 1992; **67**: 594-9.
2) Sadler JE. Biochemistry and genetics of von Willebrand factor. Annu Rev Biochem 1998; **67**: 395-424.
3) Wagner DD. Cell biology of von Willebrand factor. Annu Rev Cell Biol 1990; **6**: 217-46.
4) Valentijn KM, Sadler JE, Valentjin JA, et al. Functional architecture of Weibel-Palade bodies. Blood 2011; **117**: 5033-43.
5) Sadler JE, Budde U, Eikenboom JC, et al. Update on the pathophysiology and classification of von Willebrand disease: a report of the Subcommittee on von Willebrand factor. J Thromb Haemost 2006; **4**: 2013-4.
6) Sadler JE. Von Willebrand factor: two sides of a coin. J Thromb Haemost 2005; **3**: 1702-9.
7) Lillicrap D. von Willebrand disease: advances in pathogenetic understanding, diagnosis, and therapy. Blood 2013; **122**: 3735-40.
8) James PD, Notley C, Hegadorn C, et al. The mutational spectrum of type 1 von Willebrand disease: results from a Canadian cohort study. Blood 2007; **109**: 145-54.
9) Goodeve A, Eikenboom J, Castaman G, et al. Phenotype and genotype of a cohort of families historically diagnosed with type 1 von Willebrand disease in the European study, Molecular and Clinical Markers for the Diagnosis and Management of Type 1 von Willebrand Disease (MCMDM-1VWD). Blood 2007; **109**: 112-21.
10) Cumming A, Grundy P, Keeney S, et al. An investigation of the von Willebrand factor genotype in UK patients diagnosed to have type 1 von Willebrand disease. Thromb Haemost 2006; **96**: 630-41.
11) Budde U, Schneppenheim R, Eikenboom J, et al. Detailed von Willebrand factor multimer analysis in patients with von Willebrand disease in the European study, molecular and clinical markers for the diagnosis and management of type 1 von Willebrand disease (MCMMDM-1VWD). J Thromb Haemost 2008; **6**: 762-71.
12) Berendsen, HJC, van der Spoel D, van Drunen D. GROMACS: a message-passing parallel molecular dynamics implementation. Comput Phys Commun 1995; **91**: 43-56.
13) Lindahl E, Hess B, van der Spoel D. GROMACS 3.0: a package for molecular simulation and trajectory analysis. J Mol Model 2001; **7**: 306-17.
14) Oostenbrink C, Villa A, Mark AE, van Gunsteren WF. A biomolecular force field based on the free enthalpy of hydration and solvation: the GROMOS force-field parameter sets 53A5 and 53A6. J Comput Chem 2004; **25**: 1656-76.
15) Shiltagh N, Kirkpatrick J, Cabrita LD, et al. Solution structure of the major factor VIII binding region of von Willebrand factor. Blood 2014; **123**: 4143-51.
16) Humphrey W, Dalke A, Schulten K. VMD - Visual Molecular Dynamics, J Molec Graphics 1996; **14**: 33-8.
17) Berendsen HJ, Postma JP, van Gunsteren WF, Hermans J. *Interaction Models for Water in Relation to Protein Hydration*. Dordrecht: Reider Publishing Company; 1981.
18) Miyamoto S, Kollman PA. Settle: an analytical version of the SHAKE and RATTLE algorithm for rigid water models. J Comput Chem 1992; **13**: 952-62.
19) Hess B, Bekker H, Berendsen HJ, Fraaije JG. LINCS: A linear constraint solver for molecular simulations. J Comp Chem 1997; **18**: 1463-72.
20) Darden TA, York D, Pedersen L. Particle mesh Ewald: An N·log(N) method for Ewald sums in large systems. J Chem Phys 1993; **98**: 10089-92.
21) Hockney RW, Goel SP, Eastwood J. Quiet high-resolution computer models of a plasma. J Chem Phys 1974; **14**: 148-58.
22) Biswal HS, Gloaguen E, Loquais Y, et al. Strength of NH·S hydrogen bonds in methionine residues revealed by gas-phase IR/UV spectroscopy. J Phys Chem Lett 2012; **3**: 755-9.
23) Chiang HY, Cohen GH, Eisenberg RJ. Identification of functional regions of herpes simplex virus glycoprotein gD by using Linker-Insertion Mutagenesis. J Virol 1994; **68**: 2529-43.
24) Goodeve AC. The genetic basis of von Willebrand disease. Blood Rev 2010; **24**: 123-34.
25) Gill JC, Endres-Brooks J, Bauer PJ, et al. The effect of ABO blood group on the diagnosis of von Willebrand disease. Blood 1987; **69**: 1691-5.
26) Keightley AM, Lam YM, Brady JN, et al. Variation at the von Willebrand factor (vWF) gene locus is associated with plasma VWF:Ag levels: identification of three novel single nucleotide polymorphisms in the vWF gene promoter. Blood 1999; **12**: 4277-83.
27) von Willebrand factor variant database (VWFdb). Available at: http://www.vwf.group.shef.ac.uk/. Accessed on 03/12/2015.
28) Bellissimo DB, Christopherson PA, Flood VH, et al. Von Willebrand factor mutations and new sequence variations identified in healthy controls are more frequent in the African-American population. Blood 2012; **119**: 2135-40.
29) Eikenboom JCJ, Vink T, Briet E, et al. Multiple substitutions in the von Willebrand factor gene that mimic the pseudogene sequence. Proc Natl Acad Sci USA 1994; **91**: 2221-4.
30) International Genome Sample Resource. 1000 Genomes - A Deep Catalog of Human Genetic Variation. Available at: http://browser.1000genomes.org/Homo_sapiens/Gene/Variation_Gene/Table?db=core;g=ENSG00000110799. Accessed on 03/12/2015.
31) Eikenboom J, Hilbert L, Ribba AS, et al. Expression of 14 von Willebrand factor mutations identified in patients with type 1 von Willebrand disease from MCMDM-1VWD study. J Thromb Haemost 2009; **7**: 1304-12.
32) Berber E, James PD, Hough C, Lillicrap D. An assessment of the pathogenic significance of the R924Q von Willebrand factor substitution. J Thromb Haemost 2009; **7**: 1672-9.
33) Hickson N, Hampshire D, Winship P, et al. von Willebrand factor variant p.Arg924Gln marks an allele associated with reduced von Willebrand factor and factor VIII levels. J Thromb Haemost 2010; **8**: 1986-93.

34) O'Brien LA, James PD, Othman M, et al. Founder von Willebrand factor haplotype associated with type 1 von Willebrand disease. Blood 2003; **102**: 549-57.

35) Davies JA, Collins PW, Hathaway LS, Bowen DJ. C1584: effect on von Willebrand factor proteolysis and von Willebrand factor antigen levels. Acta Haematol 2009; **121**: 98-101.

36) Keeney S, Grundy P, Collins PW, Bowen DJ. C1584 in von Willebrand factor is necessary for enhanced proteolysis by ADAMTS13 in vitro. Hemophilia 2007; **13**: 405-8.

37) Rawley O, O'Sullivian JM, Chion A, et al. von Willebrand factor arginine 1205 substitution results in accelerated macrophage-dependent clearance in vivo. J Thromb Haemost 2015; **13**: 821-6.

38) Castaman G, Lethagen S, Federici AB, et al. Response to desmopressin is influenced by the genotype and phenotype in type I von Willebrand disease (VWD): results from the European Study MCMDM-1 VWD. Blood 2008; **111**: 3531-9.

39) Riddell AF, Gomez K, Millar CM, et al. Characterization of W1745C and S1783A: 2 novel mutations causing defective collagen binding in the A3 domain of von Willebrand factor. Blood 2009; **114**: 3489-96.

40) Flood VH, Lederman CA, Wren JS, et al. Absent collagen binding in a VWF A3 domain mutant: utility of the VWF:CB in diagnosis of VWD. J Thromb Haemost 2010; **8**:1431-3.

41) Castaman G, Giacomelli SH, Jacobi PM, et al. Reduced von Willebrand factor secretion is associated with loss of Weibel-Palade body formation. J Thromb Haemost 2012; **10**: 951-8.

42) Bodo I, Katsumi A, Tuley EA, et al. Type 1 von Willebrand disease mutation Cys1149Arg causes intracellular retention and degradation of heterodimers: a possible general mechanism for dominant mutations of oligomeric proteins. Blood 2001; **98**: 2973-9.

43) Haberichter SL, Castaman G, Budde U. Identification of type 1 von Willebrand disease patients with reduced von Willebrand factor survival by assay of the VWF propeptide in the European study: molecular and clinical markers for the diagnosis and management of type 1 VWD (MCMDM-1VWD). Blood. 2008; **15**: 4979-8.

Correspondence: Ergül Berber
Moleküler Biyoloji ve Genetik Bölümü
İstanbul Arel Üniversitesi
Tepekent Büyükçekmece
34357 İstanbul, Turkey
e-mail: ergulberber@arel.edu.tr